Grayanotoxin-I-modified Eel Electroplax Sodium Channels

Correlation with Batrachotoxin and Veratridine Modifications

DANIEL S. DUCH, ALLISON HERNANDEZ, SIMON R. LEVINSON, and BERND W. URBAN

From the Departments of Anesthesiology and Physiology, Cornell University Medical College, New York 10021; Department of Physiology, University of Colorado Medical College, Denver, Colorado 80262; and Institut für Anästhesiologie, Universität Bonn, D5300 Bonn 1, Germany

ABSTRACT To probe the structure–function relationships of voltage-dependent sodium channels, we have been examining the mechanisms of channel modification by batrachotoxin (BTX), veratridine (VTD), and grayanotoxin-I (GTX), investigating the unifying mechanisms that underlie the diverse modifications of this class of neurotoxins. In this paper, highly purified sodium channel polypeptides from the electric organ of the electric eel were incorporated into planar lipid bilayers in the presence of GTX for comparison with our previous studies of BTX (Recio-Pinto, E., D. S. Duch, S. R. Levinson, and B. W. Urban. 1987. *J. Gen. Physiol.* 90:375–395) and VTD (Duch, D. S., E. Recio-Pinto, C. Frenkel, S. R. Levinson, and B. W. Urban. 1989. *J. Gen. Physiol.* 94:813–831) modifications. GTX-modified channels had a single channel conductance of 16 pS. An additional large GTX-modified open state (40–55 pS) was found which occurred in bursts correlated with channel openings and closings. Two voltage-dependent processes controlling the open time of these modified channels were characterized: (*a*) a concentration-dependent removal of inactivation analogous to VTD-modified channels, and (*b*) activation gating similar to BTX-modified channels, but occurring at more hyperpolarized potentials. The voltage dependence of removal of inactivation correlated with parallel voltage-dependent changes in the estimated $K_{1/2}$ of VTD and GTX modifications. Ranking either the single channel conductances or the depolarization required for 50% activation, the same sequence is obtained: unmodified > BTX > GTX > VTD. The efficacy of the toxins as activators follows the same ranking (Catterall, W. A. 1977. *J. Biol. Chem.* 252:8669–8676).

INTRODUCTION

In this paper we continue our examination of the molecular functions of voltage-dependent sodium channels, probing the interactions of the purified sodium channel polypeptide from the electric organ of the electric eel with the lipid soluble neurotoxins batrachotoxin (BTX), veratridine (VTD), and grayanotoxin-I (GTX). These toxins bind competitively to the channel protein (Catterall, 1977) and cause significant alterations in almost all measured channel functions (Strichartz, Rando, and Wang, 1987; Brown, 1988). The toxin binding site may therefore be part of, or allosterically connected with, a key structural element mediating or participating in voltage-dependent changes in channel conformation (Brown, 1988). In spite of the similarities among the toxins, however, many differences have been reported in their macroscopic modifications of channel function (Khodorov, 1985). The toxins thereby provide natural tools for studying and mapping the structure–function correlations of the toxin binding microenvironment (Brown, 1988). Furthermore, as all of these modifiers have a much higher affinity for the open conformation of the channel than for its nonconducting states (Khodorov, 1985), they specifically may provide structural information about this transient conducting conformation of the channel.

A necessary step in the investigation of these structure–function relationships is the comparative characterization of the properties of the channel when it is modified by the various toxins under identical experimental conditions, an approach analogous to that used in the examination of the pharmacological properties of these toxins (Catterall, 1977). The experiments presented in this series of papers, which include our previous examinations of BTX- (Recio-Pinto, Duch, Levinson, and Urban, 1987) and VTD- (Duch, Recio-Pinto, Frenkel, Levinson, and Urban, 1989) modified channels, are thus directed toward understanding sodium channel function through the characterization of functional toxin interactions with purified, single sodium channel proteins under the experimentally controlled conditions afforded by planar lipid bilayer methodology.

In this paper we describe the single channel conductance and activation properties of GTX-modified electroplax sodium channels in planar bilayers. Among this group of lipid soluble toxins, GTX is the only nonalkaloid channel modifier (Catterall, 1980). After describing and comparing the modifications of the eel sodium channels by GTX, BTX, and VTD, we examine our results with respect to proposed models of toxin–channel binding interactions.

A preliminary report of some of this work has been presented (Duch, Levinson, and Urban, 1991).

MATERIALS AND METHODS

Preparation of Sodium Channels

Sodium channels from *Electrophorus electricus* were solubilized with the detergent CHAPS (3-[3-cholamidopropyl]-dimethylammonio-1-propane sulfonate; Calbiochem Corp., La Jolla, CA), purified, and reconstituted into lipid vesicles as previously described (Duch and Levinson, 1987a; Recio-Pinto et al., 1987). Reconstituted channels from four separate purifications were used, as described in our previous studies (Table I of Duch et al., 1989).

Planar Bilayer Measurements

Most experimental methods and materials were as described elsewhere (Recio-Pinto et al., 1987; Duch et al., 1988, 1989); a brief review is presented here.

All experiments were conducted at room temperature (22–27°C) in symmetrical 500 mM NaCl buffered at pH 7.4 with 10 mM HEPES (United States Biochemical Corp., Cleveland, OH); no corrections were made for temperature differences between experiments. Tetrodotoxin (TTX) and VTD were purchased from Sigma Chemical Co. (St. Louis, MO); GTX was kindly given by Dr. T. Narahashi (Northwestern University Medical School, Evanston, IL). Planar bilayers were formed from neutral phospholipid solutions containing (4:1) 1-palmitoyl-2-oleoyl-phosphatidylethanolamine and 1-palmitoyl-2-oleoyl-phosphatidylcholine (Avanti Polar Lipids, Inc., Birmingham, AL) in decane (5% wt/vol, 99.9% pure; Wiley Organics, Columbus, OH).

Teflon bilayer chambers were designed, prepared, and cleaned as previously described (Recio-Pinto et al., 1987). These chambers were divided into two compartments, a *cis* side to which the reconstituted preparation was added, and a *trans* side. Sodium channels were incorporated into bilayers in the presence of 5 or 40 μM GTX or 5 μM VTD, present in both chambers, as described (Levinson, Duch, Urban, and Recio-Pinto, 1986). In some experiments, channels were incorporated in the presence of 5 μM GTX and the toxin concentration was subsequently increased to 40 μM after initial experiments conducted at the lower concentration. When channels incorporated asymmetrically in the bilayer (Duch et al., 1989) 25–50 μM TTX was added to one of the chambers to block channels in one direction; the electrophysiological sign convention was used in the presentation of results.

Channel currents were recorded under voltage-clamp conditions using a standard current-to-voltage amplifier. Strip chart records were typically filtered at 50 Hz (8-pole Bessel), and single channel current transitions were measured by hand from these records. Slope conductances were obtained using linear regression analysis of current–voltage curves between −100 and +100 mV.

The durations of preopening and preclosing bursts were also measured by hand from the strip chart records. Only bursts that had clearly defined starting and ending points (i.e., no prolonged [>100 ms] closures during the burst) were used for the open-time distribution analyses. Open times were grouped in 100-ms bins.

Measurement of the Voltage Dependence of Channel Conductance

To measure the voltage dependence of channel conductance, the bilayer was clamped to +100 mV for at least 60 s. The membrane was then hyperpolarized in sequential −10-mV steps to a final potential between −100 and −150 mV, before being depolarized with sequential +10-mV steps back to +100 mV. Each potential was held for either 4 or 31.5 s and the initial 2.5 or 30 s, respectively, of the currents was recorded by computer. These currents (I_t) were composed of currents from three sources:

$$I_t = I_{Na} + I_c + I_b$$

where I_{Na} is the current through sodium channels, I_c is a faster capacitative transient (lasting ~1 s or less), and I_b is the background current.

I_c was removed by subtracting the current trace at 0 mV from I_t at all potentials by computer. I_b was a combination of leak current through the bilayer and slower (seconds to minutes) capacitative transients not subtracted with the 0-mV trace. To measure I_b, at least three control curves (two 4-s and one 31.5-s protocols) were recorded in the absence of toxin or sodium channels. The experimental toxin, GTX or VTD, was then added to the chamber and three more control curves were recorded. An average background conductance ($g_b = I_b/V_h$, where V_h

is the holding potential) of <5–15 pS was verified before any channel material was added. This conductance was usually stable and did not change significantly during an experiment. To confirm this, the background conductances measured for each holding potential were compared with the experimental conductances recorded at potentials where all channels were closed. In addition, background parameters were sometimes measured when channels were either no longer observed in the bilayer, or after the addition of 50 μM TTX to the channels to block all transitions. If a change in the background parameters was observed, the control values were adjusted. I_b at each potential was time-averaged by computer and subtracted from $(I_t - I_c)$ at the corresponding potentials to obtain I_{Na}. I_{Na} was then converted to conductance (g_{Na}). This procedure determined the background conductance more rigorously than in our previous experiments (Duch et al., 1989). For comparative purposes in some figures, our previous data (Duch et al., 1989) were reanalyzed according to this newer procedure.

Steady-State Activation Gating

Steady-state activation was examined by holding channels at a depolarized potential (+100 mV) for at least 60 s, before jumping to a hyperpolarized potential of −100 to −150 mV. The membrane was then sequentially depolarized in +10-mV steps back to +100 mV. Background currents were measured and subtracted as described above. Channel fractional open time (f_o) was calculated as previously described for BTX-modified channels (Recio-Pinto et al., 1987; Duch et al., 1988). The gating data were fitted to a Boltzmann distribution with one open and one closed state, as described (Recio-Pinto et al., 1987). Because channels generally closed by inactivation (see below) before reaching $f_o = 1$, several gating measurements on the same membranes and channels were combined and averaged to obtain a complete curve. Due to the inherent variability of the gating properties of these channels (Recio-Pinto et al., 1987), and because some of these membranes contained multiple channels, this analysis provides only a lower limit to the determination of the effective valence (Levinson et al., 1986).

RESULTS

Single Channel Conductance in Symmetrical Sodium Solutions

In the presence of GTX, sodium channels from the eel electroplax had a conductance of 14–16 pS (Fig. 1, A and B). This conductance is smaller than that of BTX-modified electroplax channels in planar bilayers (25 pS; Recio-Pinto et al., 1987), but larger than the same channels modified with VTD and recorded under identical conditions (10–12 pS; Duch et al., 1989). As previously described with BTX and VTD, these channels exhibit functional heterogeneity, with smaller channel conductances also present. These smaller conductance transitions were about half the size of the larger channel conductance (6–8 pS), and were usually observed in the presence of the larger conductance (Fig. 1 C), but rarely alone (Fig. 1 D).

Under symmetrical salt conditions, GTX-modified channels had approximately linear current–voltage $(I-V)$ relationships which were symmetrical between −100 and +100 mV (Fig. 2 A), as was found with channels modified with BTX and VTD (Recio-Pinto et al., 1987; Duch et al., 1989). The average slope conductance in this voltage range, determined from linear regression fits of channel $I-V$ curves from 10 membranes, was 15.5 pS (SEM = ±0.5 pS; $n = 10$; 24–27°C). The smaller conductances also had linear and symmetrical $I-V$ relationships (Fig. 2 B). From five membranes where the smaller conductances could be readily measured at several potentials, the averaged slope conductance was 7.4 pS (±0.5 pS).
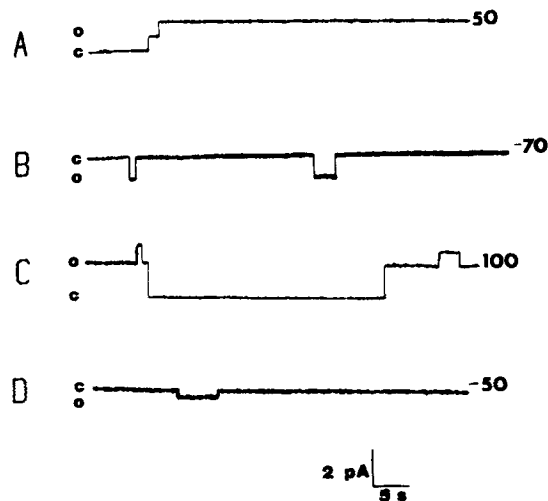
A o
   c ⎽⎽⎽⎽⎽⎽⎽⎽⎽⎽⎽⎽⎽⎽⎽⎽⎽⎽⎽⎽⎽**50**

B c
   o ⎽⎽⎽⎽⎽⎽⎽⎽⎽⎽⎽⎽⎽⎽⎽⎽**-70**

C o ⎽⎽⎽⎽⎽⎽⎽⎽⎽⎽⎽⎽⎽⎽⎽⎽**100**
   c

D c ⎽⎽⎽⎽⎽⎽⎽⎽⎽⎽⎽⎽⎽⎽⎽⎽**-50**
   o

2 pA
9 s

FIGURE 1. GTX-modified single channel transitions of eel electroplax sodium channels in symmetrical 500 mM NaCl. All traces were recorded at 50 Hz in the presence of 40 μM GTX. (A) Trace from a membrane containing at least two channels of 14 and 15 pS; holding potential was +50 mV. (B) Trace from a membrane containing at least seven channels; holding potential was −70 mV. All the channels except one (18 pS) are closed at this potential; the channel is closed most of the time. (C) Trace recorded from a membrane containing at least one 17-pS channel and an 8-pS channel; holding potential was +100 mV. (D) Trace from a membrane containing a 6–7-pS channel without any larger channels present; holding potential was −50 mV.
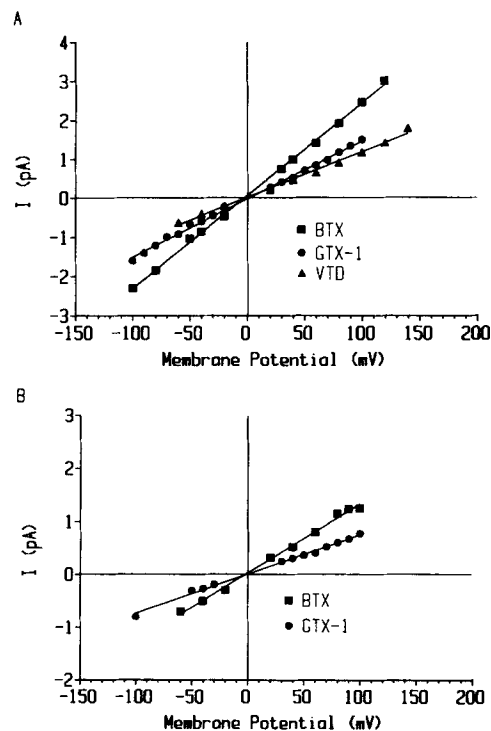
A

B

FIGURE 2. *I-V* relationships of GTX-modified channels between −100 and +100 mV. (A) GTX-modified channel (*circles*) *I-V* relationship in 500 mM NaCl compared with BTX (*squares*) and VTD (*triangles*) channels. GTX data are the average from 10 membranes, ±SEM; a linear regression fit of the data yielded a slope conductance of 14.8 pS, r^2 = 0.998. The BTX and veratridine curves are from Recio-Pinto et al., 1987, and Duch et al., 1989, respectively. (B) GTX-modified channel with smaller conductance. The slope conductance of the GTX *I-V* curve (*circles*) is 7.4 pS (r^2 = 0.995). An example of a small BTX channel (12 pS) is given for comparison (*squares*).
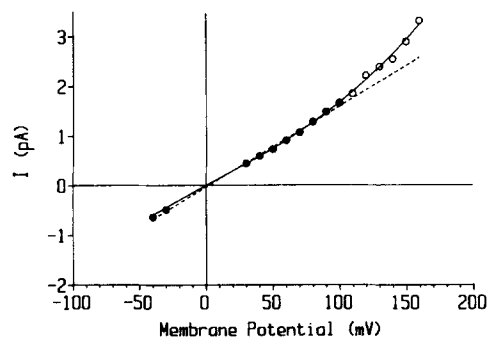
FIGURE 3. The GTX-modified channel conductance was markedly superlinear at potentials larger than ±100 mV. The dashed line is a linear regression fit of the data between −100 and +100 mV (*filled circles*). The slope conductance for the data between −100 and +100 mV was 16.2 pS, $r^2 = 0.997$. For demonstration, all data (*filled and open circles*) were fitted with a polynomial:

$$I = aV + cV^3$$

where $a = 14.5$ pS and $c = 2.23 \times 10^{-7}$ pS/mV^2.

At potentials greater than −100 or +100 mV, the I-V relations became markedly superlinear (Fig. 3). Such marked superlinearity was not obvious when either BTX or VTD was used as a channel modifier.

High Conductance State

In addition to the 16-pS conductance, sodium channels modified with GTX sometimes opened transiently to a conductance state of 40–55 pS (Fig. 4). No corresponding large conductances were observed in experiments using either BTX or VTD as a
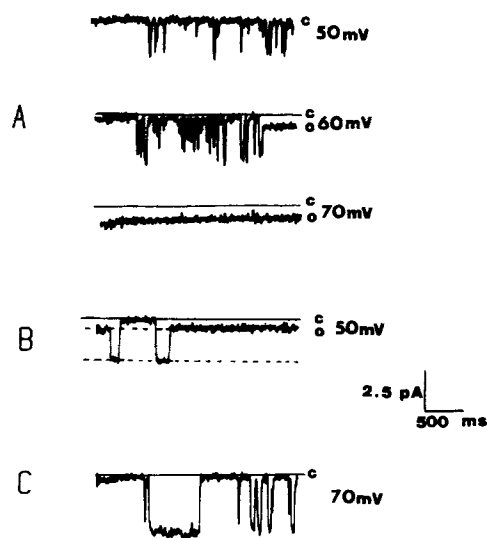

FIGURE 4. Transient opening of GTX-modified channels to a conductance of 40–55 pS. (*A*) Three sequentially recorded traces from a membrane being depolarized in 10-mV steps from negative holding potentials. Each potential was held for 4 s and the first 2.5 s of each trace are displayed, after the subtraction of the fast capacitative transient. No channel was open in the membrane until the potential reached +50 mV (*top trace*), when transitions to a large conductance state began (preopening burst). These large transitions continued until the channel opened to a more stable 15-pS conductance level (*second trace*, +60 mV); the 15-pS opening remained stable and no further large transitions were observed in this experiment (*bottom trace*, +70 mV). (*B*) These large openings could occur before channel openings or closings. In this trace, a channel is open with a 15-pS conductance, then converts to a 55-pS conductance level before closing. It subsequently reopens to the 55-pS level before returning to the 15-pS conductance state. Recorded at +50 mV. (*C*) The larger conductance state was also (rarely) found to be stable for up to 1 s without converting to the 15-pS conductance level; +70 mV. All traces were filtered at 50 Hz.

modifier. These high conductance states usually occurred in bursts either when a channel changed from a nonconducting state to the more stable open (16 pS) state (preopening bursts), or when a channel went from this stable open state back to a nonconducting state (preclosing bursts). On rare occasions, this high conductance state was stable for > 1 s (Fig. 4).

The bursts were observed at all holding potentials. However, the proportion of channel openings and closings preceded by these bursts increased with increasing depolarization of the membrane (Fig. 5), representing a significant fraction of channel openings and closings only at positive potentials. At positive potentials, the bursts occurred 40–50% less frequently before channel closings (Fig. 5 *B*) than before
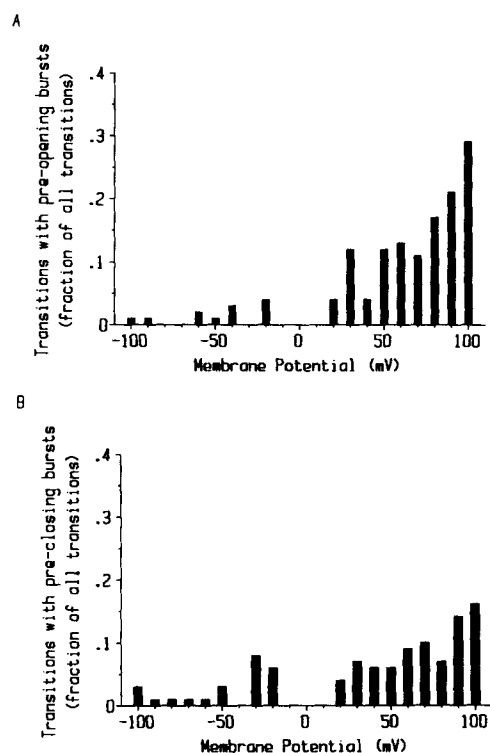
A

B

FIGURE 5. The large conductance bursts were voltage dependent. (*A*) The fraction of channel openings (2,458 total transitions) and (*B*) closings (2,343 total transitions) preceded by these large bursts, as a function of potential. The large preopening busts occurred 1.8–2 times more frequently than preclosing bursts.

channel openings (Fig. 5 *A*). The total fractions of observed preopening (0.22 and 0.23) and preclosing bursts (0.14 and 0.17) were independent of toxin concentration at 5 and 40 μM GTX, respectively.

The purity of our toxin samples was undetermined, and the quantities available were too small for both adequate analysis and experimentation. Nonetheless, several lines of evidence lead us to conclude that these high conductances represent a GTX-modified state. First, these high conductance states were observed in all membranes with GTX-modified channels and with all GTX concentrations used (5–180 μM). Second, they were never observed during the control periods of any experiment, when the toxin was present but before sodium channels were added; nor were they observed when channels were added to the chamber in the absence of GTX

(>8 h recording time). Third, in all experiments where TTX was added to the experimental chamber to block sodium channels, these high conductance states were also blocked. Finally, their correlation with both 16-pS conductance openings and closings, as well as their greater association with channel openings compared with closings, make their attribution to a contaminant in the GTX preparation highly unlikely.

The open-time distributions for these GTX-modified preopening and preclosing bursts were surveyed at +100 mV in order to examine if these bursts might be occurring before all current transitions, but were not observed because of the low experimental bandwidth (50 Hz). These open-time distributions were well described by single exponential decays within the time range of 100 ms to seconds (Fig. 6). The
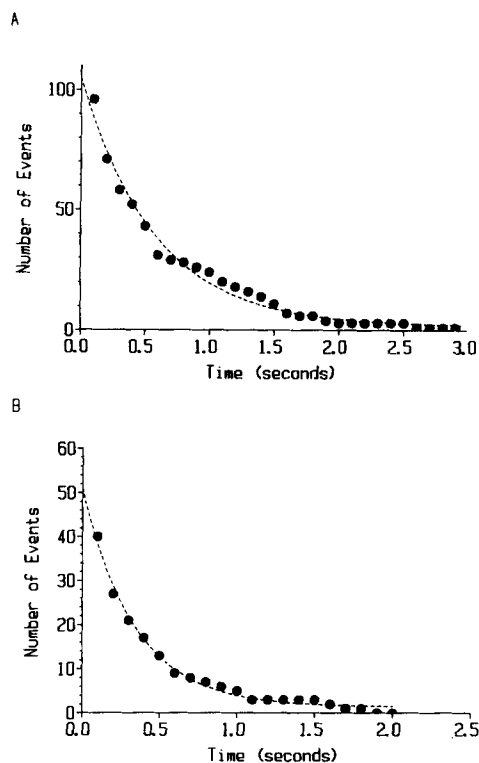

FIGURE 6. Cumulative lifetime distributions of preopening (A) and preclosing (B) bursts at +100 mV. The open-time distributions were described by single-exponential decays. $t_{1/2} = 398$ ms; $N_{(t=0)} = 103$ (preopening bursts); $t_{1/2} = 236$ ms; $N_{(t=0)} = 50$ (preclosing bursts).

$t_{1/2}$ of the preclosing bursts was shorter than that of the preopening bursts. Although higher frequency recordings will be needed to confirm these observations, our results gave no indication that a significant number of bursts within this population were missed under our recording conditions. The presence of a second population of large conductance bursts with a faster time constant also cannot be ruled out. It therefore appears that the 16-pS GTX-modified open state of the channel can be activated from at least two separate pathways (from a nonconducting state to the 16-pS open state, and from the large conductance state to the 16-pS state). The number of bursts occurring at other potentials was too small for a similar statistical examination of

open-time distributions. The significance of this large conductance state will be discussed below.

Voltage-dependent Regulation of Modified Channel Openings

The fractional open time of GTX-modified channels was voltage dependent, exhibiting characteristics of both BTX- and VTD-modified channels. Similar to VTD, GTX-modified channels had a shallow, voltage-dependent behavior, with both the number of channels open at any time and the duration of channel open time increasing with membrane depolarization (Fig. 7A). This process occurred at potentials where sodium channels are normally inactivated, and therefore, we suggest, represents a toxin-modified removal of inactivation. Superimposed on this removal of inactivation was a voltage-dependent activation gating of the channels (Fig. 7 B), which represented a more rapid cycling between the open and a closed (resting) channel state than did the removal of inactivation. This gating occurred only at very hyperpolarized potentials (< -50 mV; see below), and probably corresponds to the activation gating previously described for BTX-modified eel channels (Recio-Pinto et al., 1987). The frequency of the open–closed transitions in the gating region, however, was lower than observed with BTX, being readily resolved at 50 Hz.

The presence and potential-dependent overlap of these two processes complicated their examination in bilayers. To examine these two processes and meaningfully compare the results with those obtained with BTX and VTD-modified eel channels, therefore, the protocols developed in our previous papers (Recio-Pinto et al., 1987; Duch et al., 1989) were modified as described in Materials and Methods.

Voltage-dependent Removal of Inactivation

Compared with VTD, GTX-modified channels characteristically had longer open and closed times at depolarized potentials (Fig. 7; compare with VTD-modified channel openings and closings in Fig. 5A of Duch et al., 1989). Because almost all membranes had more than one channel (51 of 52 membranes with channels), a detailed analysis of the averaged open and closed times of GTX-modified channels was not possible. The results from the only single channel membrane (in which no other channels appeared for > 120 min recording time) are shown in Table I. It can be seen that even at very depolarized potentials, where the channel fractional open time was > 0.9, long closures (> 60 s) occurred; such long duration closures were not observed with VTD-modified channels (Duch et al., 1989, Table II, 5 μM VTD), which had closures averaging < 3 s at all potentials where the channel fractional open time was > 0.5. A population of similar short duration closures was also observed with GTX, but less frequently (Table I), contributing little to the fractional closed time of GTX-modified channels. At the same fractional open times, GTX-modified channels also have much longer t_o's than VTD-modified channels (Fig. 5 and Table II of Duch et al., 1989). Closures of both long and short duration were observed in all membranes and with all GTX concentrations used (5–180 μM).

Because of the relatively long duration closures observed with GTX, the fractional open time (f_o) of the GTX-modified channels was always < 1, even at very depolarized (> 100 mV) potentials. Therefore, the number of channels in almost all membranes could not be determined with certainty, and f_o could not be measured
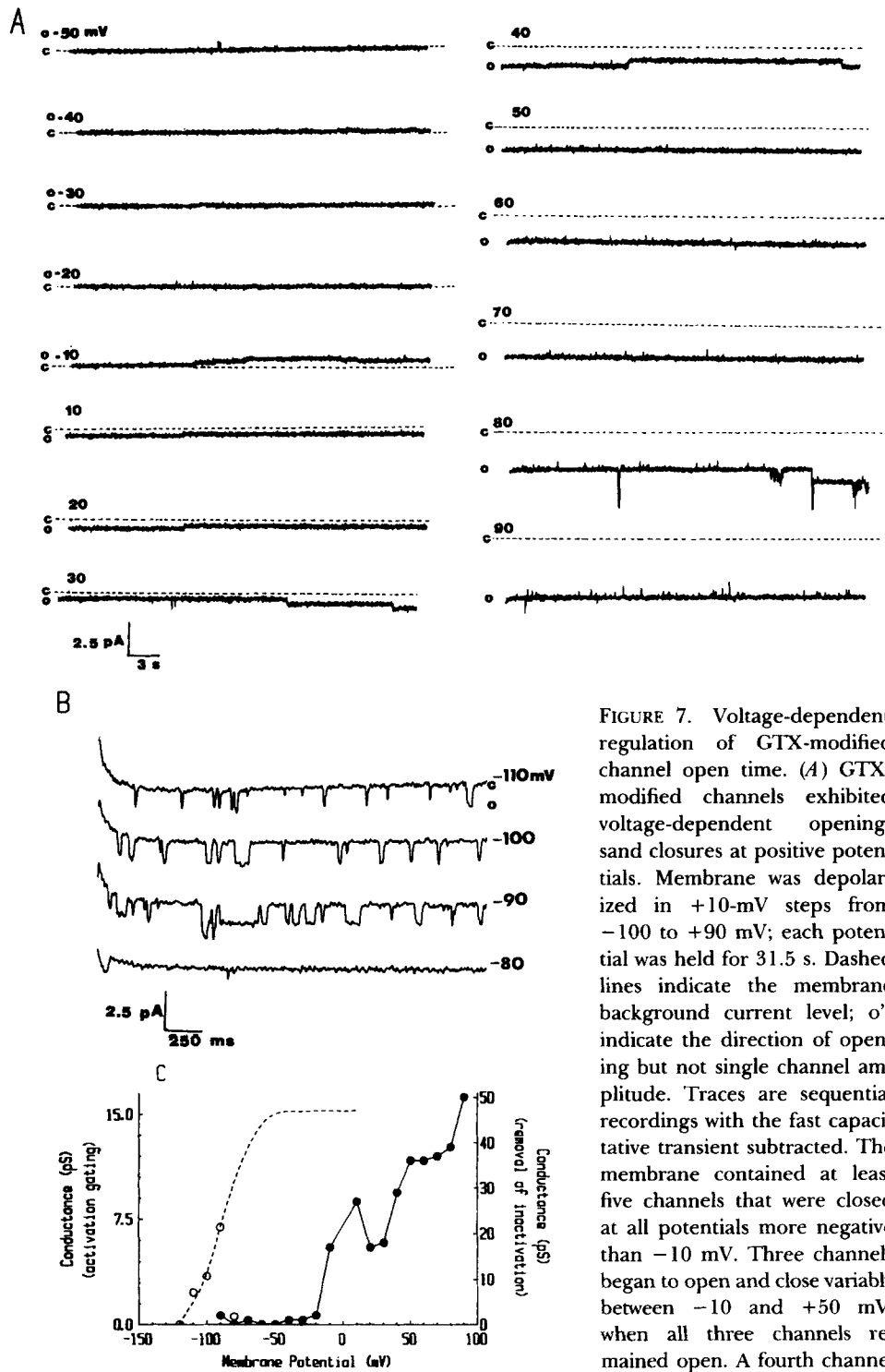
THE JOURNAL OF GENERAL PHYSIOLOGY · VOLUME 100 · 1992

FIGURE 7. Voltage-dependent regulation of GTX-modified channel open time. (*A*) GTX-modified channels exhibited voltage-dependent openings and closures at positive potentials. Membrane was depolarized in +10-mV steps from −100 to +90 mV; each potential was held for 31.5 s. Dashed lines indicate the membrane background current level; o's indicate the direction of opening but not single channel amplitude. Traces are sequential recordings with the fast capacitative transient subtracted. The membrane contained at least five channels that were closed at all potentials more negative than −10 mV. Three channels began to open and close variably between −10 and +50 mV, when all three channels remained open. A fourth channel

TABLE I

Averaged Open and Closed Times for Single Channel

V_m	t_o	t_c	$t_{c1}(>5$ s$)$	$t_{c2}(<5$ s$)$
		s		
+80	265.3 ± 83.0(4)	52.5(2)	103(1)	2.0(1)
+60	94.3 ± 39.8(8)	25.8 ± 15.5(6)	74(2)	1.6 ± 0.5(4)
+40	103.0 ± 10.3(6)	45.5 ± 15.8(5)	56.0 ± 14.8(4)	2.0(1)
+20	15.5 ± 5.3(3)	186.3 ± 88.9(3)	186.3 ± 88.9(3)	—

Averages are from one membrane, recorded for >2 h without any additional sodium channel incorporations. V_m is the holding potential (millivolts); t_o is the averaged time between channel closings; t_c is the averaged time between channel openings. For illustration, closures contributing to t_c were separated into two groups: closures >5 s (t_{c1}) and closures <5 s (t_{c2}). Data are the average and SEM of up to eight events (the number of events contributing to each average is given in parentheses). No channel openings were observed at potentials more hyperpolarized than +20 mV (10–20 min recording per potential).

directly. The voltage dependence of this removal of inactivation was therefore examined by normalizing the channel conductance to that recorded at +90 mV and averaging between membranes (Figs. 8–10).

In spite of the differences in the duration of GTX- and VTD-modified open and inactive states, the steady-state voltage dependence of the removal of inactivation was remarkably similar with both toxins (Fig. 8); the only apparent difference occurred at low membrane potentials around ±10 mV. This suggested that the underlying molecular processes controlling the voltage-dependent removal of inactivation were the same with both toxins. However, as might be expected from the longer duration openings and closures, GTX-modified channels took longer to reach the steady state ($\sim$30 s/potential; Fig. 9, *A* and *B*) than VTD-modified channels ($\sim$4 s/potential; Fig. 9 *C*).

This voltage-dependent removal of inactivation might result directly from voltage-dependent toxin binding and unbinding, from a cycling between a modified open and a modified inactive state, or both. To examine the role that toxin binding plays in this process, the voltage dependence of inactivation removal was examined at lower toxin concentrations (Fig. 10). For GTX (Fig. 10, *A* and *B*), it can be seen that

opened at +80 mV, preceded by some transitions to the higher (40–55 pS) conducting state. This channel remained open at +90 mV, making a total of four channels open at this potential. A fifth channel opened after holding the membrane at +100 mV for $\sim$3 min (data not shown); 50 Hz, 5 μM GTX. (*B*) Activation gating of GTX-modified channels. This series of traces was obtained by holding the membrane at +100 mV and then clamping the potential to −120 mV before sequentially depolarizing the membrane in +10-mV steps (40 μM GTX); each potential was held for 4 s. It appears that only one channel is gating at most potentials; a second channel opened briefly at −90 mV. All channels were closed by −80 mV, probably by the slow, weakly voltage-dependent process, a typical occurrence at these potentials. (*C*) Comparison of the voltage dependence of channel activation (*open circles*) and the removal of inactivation (*closed circles*). The time-averaged conductances of the membranes in *A* and *B* were calculated by computer and plotted versus potential. For illustration, the solid line is drawn point-to-point and the dashed curve is a fit of the data between −90 and −110 mV with a two-level Boltzmann distribution ($Va = -88$ mV; $za = 2.4$).

the steady-state took longer to be reached with 5 μM GTX than with 40 μM GTX, much longer than the 30-s recording times. The time to reach the steady state was prohibitively long for determination (estimated >5 min/potential) with our system. Thus, the conductance values we used to calculate the $K_{1/2}$ of toxin modification of the channel (see below) represent our best estimate of the equilibrium values at this toxin concentration. In contrast, at lower VTD concentrations (5 μM; Fig. 10 C, open and filled circles) the removal of inactivation was still close to the steady state, and no significant hysteresis was observed with 4-s potential durations. However, the voltage dependence of inactivation removal was shifted to more depolarized potentials compared with the 50 μM VTD experiments (open triangles), indicating that VTD binding and unbinding still contributed to this process. With both GTX and VTD, therefore, these results suggest that toxin binding is in itself a voltage-dependent process, with the toxins binding more strongly at depolarized potentials and unbinding more readily at hyperpolarized potentials.
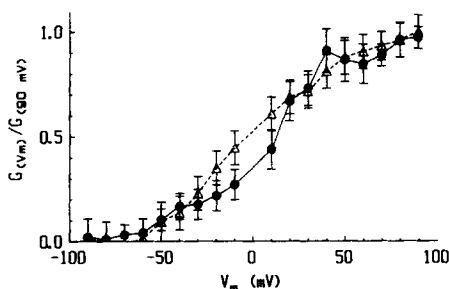

FIGURE 8. Potential-dependent steady-state removal of sodium channel inactivation by GTX (40 μM, *circles*) and VTD (50 μM, *triangles*). Membranes were held at +100 mV and sequentially hyperpolarized in −10-mV steps to −100 (VTD) or −150 mV (GTX). Membranes were then depolarized in +10-mV steps back to +100 mV. The conductances were normalized to the conductance measured at +90 mV during the hyperpolarizing sequence, and the combined hyperpolarizing and depolarizing data averaged at each potential for each toxin. Potentials were held for 4 s (VTD, data from Fig. 6 of Duch et al., 1989) or 31.5 s (GTX, average of five membranes).

The results also suggest that VTD association and dissociation rates are more rapid than GTX binding rates. However, because the time needed to reach a steady-state binding equilibrium is dependent on toxin concentration, it is possible that the time difference in reaching the GTX and VTD steady-state removals of inactivation is reflective of widely different effective toxin concentrations (i.e., $K_{1/2}$ of GTX binding may be much larger than VTD). To examine this question, the $K_{1/2}$ of GTX and VTD inactivation removal at most experimental potentials was determined from the data in Figs. 9 and 10 using the binding equilibrium equation as described in the Appendix. For this calculation, however, conductance measurements should necessarily be made at the steady state. Although the 40 μM GTX data were obtained close to equilibrium (Fig. 9 B), the 5 μM data were not, and the estimated time necessary to reach equilibrium for these experiments was prohibitive under our recording conditions. The equilibrium conductance for 5 μM GTX was therefore estimated by averaging the results of the ascending and descending 31.5-s protocols as the most objective experimental estimate available. Only data from the three experiments where conductances were determined on the same membranes with both 5 and 40 μM GTX were used (Fig. 11, filled circles). From the linear regression fit of these data,

the estimated $K_{1/2}$ of GTX binding at -40 mV was ~ 80 μM, which is similar to that measured by Narahashi and Seyama (1974; 41 μM) for GTX activation of squid axon sodium channels at the resting potential.

Assuming that incorporation rates will be similar for the two concentrations of toxin used experimentally, a similar estimate can be made for VTD binding. The
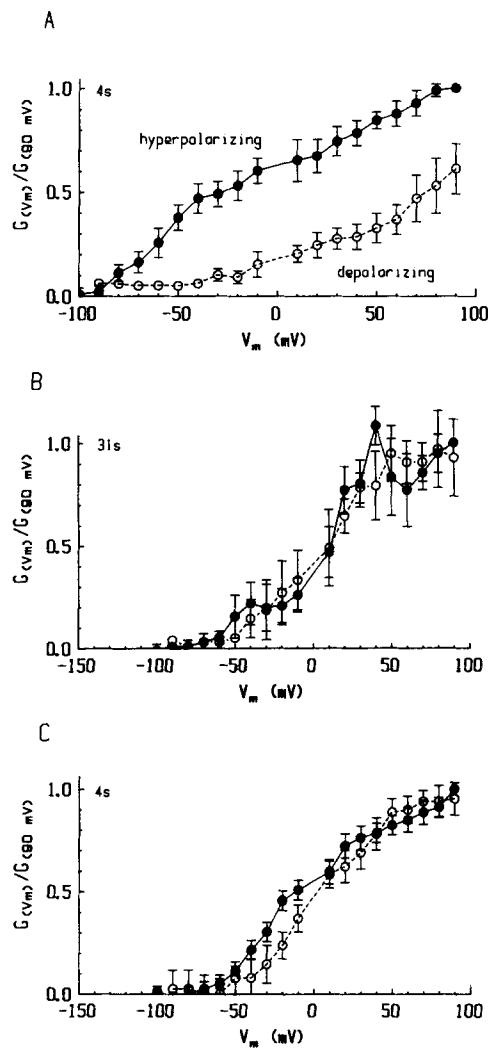

FIGURE 9. Voltage-dependent removal of sodium channel inactivation by 40 μM GTX (*A* and *B*) or 50 μM VTD (*C*). Membranes were held at $+100$ mV and sequentially hyperpolarized (*filled circles*) in -10-mV steps to -100 mV (or lower). The membrane was then depolarized in $+10$-mV steps back to $+100$ mV (*open circles*). Potentials were held for 4 s (*A*, GTX, average of 7 membranes; *C*, VTD, average of 10 membranes) or 31.5 s (B, GTX, average of 5 membranes); data were normalized to the measured conductance at $+90$ mV during the hyperpolarizing sequence. All of the membranes used in the 30-s experiments were also used in the 4-s experiments; three of these membranes were first recorded in the presence of 5 μM GTX and are included in Figs. 10 and 11. The protocol-dependent hysteresis found with GTX-modified channels and 4-s holding times was no longer evident when the membranes were held for 31.5 s in the presence of 40 μM GTX. VTD-modified channels showed only a slight hysteresis at low negative potentials when potentials were held for 4 s (*C*). The averaged hyperpolarizing and depolarizing data from *B* and *C* are shown in Fig. 8.

results of this analysis are also presented in Fig. 11 (open circles). The estimated $K_{1/2}$ of VTD binding at 0 mV (from linear regression analysis) is 5 μM, which is similar to our previous estimate of 14 μM at this potential, obtained using tracer uptake studies on purified, reconstituted eel channels (Duch and Levinson, 1987*a*).

It can be seen that the voltage dependence of VTD parallels that of GTX, although the GTX $K_{1/2}$ is about four times higher (e.g., 19 μM GTX vs. 5 μM VTD at 0 mV).

The fractions of the applied potential (calculated as described in Levinson et al., 1986) that affect GTX and VTD are −0.95 and −0.97, respectively.

Although the estimated $K_{1/2}$ of GTX binding is larger than VTD at all potentials, the toxin concentration ranges used in our experiments preclude the assignment of the measured time differences in the approach to a steady state to these differences
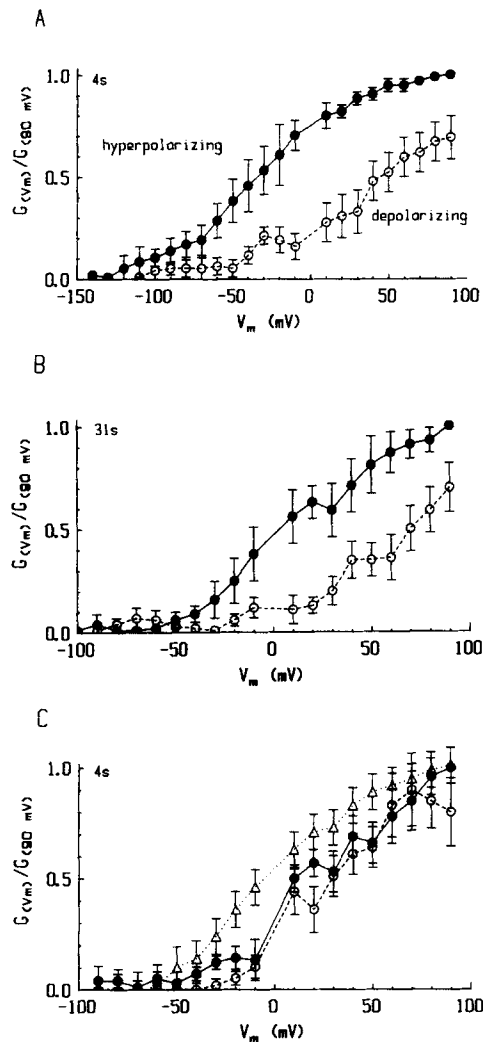

FIGURE 10. Voltage-dependent removal of inactivation of sodium channels modified with 5 μM GTX (A and B) or VTD (C). The same experimental protocol described in Fig. 9 was used; filled circles represent the hyperpolarizing sequence, open circles the subsequent depolarizing sequence. Potentials were held for 4 s (A, GTX, average of 11 membranes; C, VTD, average of 8 membranes) or 31.5 s (B, GTX, average of 8 membranes). All membranes used for the 31.5-s GTX experiments were also used in the 4-s GTX experiments. A time-dependent hysteresis in the voltage-dependent behavior was evident with both pulse durations, but dissipated slightly with longer holding times. No hysteresis is evident with 5 μM VTD, but the voltage dependence of channel open time is shifted compared with the 50-μM open times (triangles). The same purified preparations examined in the 50-μM data were used in the 5-μM experiments.

in toxin affinity. It thus appears from this analysis that the kinetics of GTX binding to the sodium channel are slower (association time constants on the order of tens of seconds) than VTD binding kinetics (association constants on the order of seconds), and may explain some of the macroscopic differences reported for modification by these two toxins (Khodorov, 1985).

Activation Gating of GTX-modified Channels

During the experiments described above, most GTX-modified channels inactivated at potentials more positive than −60 to −70 mV (Figs. 9 and 10). However, some of the channels that remained open at more negative potentials began to undergo frequent transitions between open and closed conductance states (Fig. 7 *B*). These frequent transitions were never observed at more positive potentials. This behavior was similar to that previously reported for BTX-modified activation gating of eel channels in bilayers (Recio-Pinto et al., 1987), which also only occurred at hyperpolarized potentials. However, the frequency of the GTX-modified transitions was much lower than with BTX modification, as indicated by their resolution at a filtering rate of 50 Hz (BTX-modified electroplax channel gating could not be fully resolved at this filtering frequency; Recio-Pinto et al., 1987).
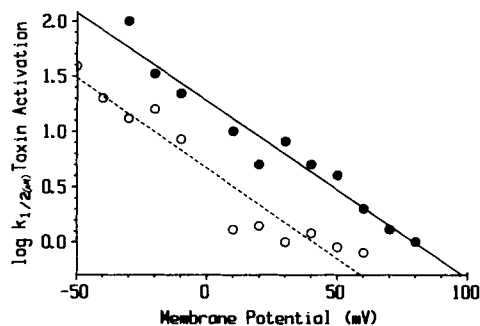

FIGURE 11. Voltage dependence of GTX and VTD binding. The effect of voltage on the $K_{1/2}$ of GTX (*filled circles*) and VTD (*open circles*) activation of sodium channels. GTX data were first obtained in the presence of 5 μM GTX before increasing the concentration to 40 μM; $K_{1/2}$ was determined from the ratio of the averaged conductances. VTD data were obtained from the experiments shown in Figs. 9 and 10. At potentials greater than +80 mV (+60 mV) with GTX (VTD) the estimated $K_{1/2}$ was well below 5 μM, making the calculations very sensitive to small experimental errors or uncertainties; these data were excluded. Below −30 mV (−50 mV) all channels were closed with the 5-μM GTX experiments, so no calculations could be made. The curves are linear regression fits to the data; r^2 = 0.95 (0.92).

To examine the voltage dependence of this activation process, channels were held in the open state at +100 mV for at least 1 min. The membrane was then stepped to a potential between −150 and −100 mV and sequentially depolarized in +10-mV steps. This pulse protocol allowed the examination of the activation process in some membranes before channels were inactivated. In most membranes, however, activation curves could not be obtained before channel inactivation and/or toxin unbinding.

GTX-modified activation gating was fit well with a two-level Boltzmann distribution (Fig. 12), similar to BTX-modified activation curves (Recio-Pinto et al., 1987). The calculated $V_{1/2}$ from four separate membranes ranged from −81 to −94 mV, with an average $V_{1/2}$ of −89.4 mV (±5.6 mV, SD; n = 4). The valence of the gating charge ranged from 6.8 to 2.6, and averaged 4.5 (±1.7, SD; n = 4).

Although these same protocols were tried with the veratridine-modified channels, no evidence of activation gating was found, perhaps indicating that either toxin unbinding or channel inactivation (or both) occurred too rapidly for observation of channel activation in the bilayer.

DISCUSSION

The most conspicuous sodium channel functions modified by the lipid-soluble toxins are the controls of inactivation and activation. Concomitant changes in channel conductance and selectivity may also add to toxin potency, but appear less critical to their efficacy. Nonetheless, these other alterations in channel function not only yield important information about the allosteric nature of sodium channel structure, but also provide tools for examining and mapping the molecular microenvironment of the toxin-binding site. By comparing the modifications of sodium channel function caused by these and related compounds, it should become possible to determine which chemical moieties are responsible for the observed modifications of sodium channels.

In the following discussion, the removal of inactivation by BTX, GTX, and VTD is compared, followed by a similar examination of the comparative effects of the toxins on single channel conductance and activation gating properties. From these compar-
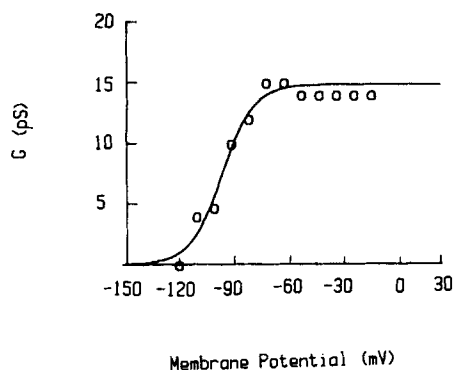

Membrane Potential (mV)

FIGURE 12. Activation gating of GTX-modified channels. The two-level Boltzmann distribution was obtained by holding the membrane at +100 mV, and then clamping the potential to -120 mV before sequentially depolarizing the membrane in +10-mV steps; each potential was held for 4 s. The data are the average of four gating sequences; at least four channels were present in the membrane, but only one gated during each measurement. The midpoint of the activation curve (V_a) was -96 mV and the valence of the apparent gating charge (z_a) was 2.8.

isons, a model describing the general molecular modifications of the sodium channel by the toxins is proposed. Finally, the binding of the toxins to the channel will be discussed in terms of previously proposed models of toxin binding.

Removal of Inactivation

In bilayer studies the removal of inactivation by BTX, GTX, and VTD is directly reflected in the measurement of channel fractional open time. With VTD and GTX, the partial removal of inactivation is reflected in the shallow, voltage-dependent increase in channel fractional open time with increasing membrane depolarization. The results presented in Figs. 9–11 present strong evidence that changes in the binding equilibria of both toxins are major determinants of this observed voltage-dependent removal of inactivation. Similar voltage-dependent differences in the binding of VTD to the sodium channel were first noted by Ulbricht (1969), and later by Sutro (1986).

This voltage-dependent toxin–channel interaction may originate from any combination of three sources: (a) a charge on the toxin molecules, or voltage-dependent sodium channel conformational changes (b) before or (c) after toxin binding. Experimental evidence indicates that the active form of BTX is the protonated (charged) species (Brown, 1988). Unfortunately, VTD and GTX have not been well characterized in this regard. If a protonated form of these toxins is responsible for the voltage-dependent binding, the charge must sense almost all of the voltage drop across the channel (0.95 to 0.97). However, Sutro (1986) stated that VTD is not charged and attributed his experimentally observed voltage-dependent VTD binding to conformational changes occurring in the channel before the toxin bound to it. According to this scheme, VTD binds only or primarily to the open state of the sodium channel, which in turn is accessible from any of several "permissive" inactive states. The transitions between these permissive states were themselves voltage dependent, and the voltage dependence of toxin binding was thus considered a consequence of the voltage-dependent availability of the open state of the channel. This scheme could at least partially explain the parallel changes in GTX and VTD binding affinities with potential, as these changes would directly depend on parallel voltage-dependent availabilities of their receptors and not on the chemical structure of the toxins. Alternatively, the toxin–channel complex could also undergo voltage-dependent conformational changes *after* binding of the toxins.

Sodium channel conformational changes have also been invoked to explain the voltage dependence of guanidinium toxin binding to the BTX-modified sodium channel (Moczydlowski, Hall, Garber, Strichartz, and Miller, 1984; Green, Weiss, and Anderson, 1987b). In this case, toxin charge was able to be ruled out as the determining factor in the observed voltage dependence, but it was not possible kinetically to distinguish between voltage-dependent conformational changes occurring either before or after toxin binding. Because GTX and VTD modify many voltage-dependent behaviors of the sodium channel, it is likely that if voltage-dependent conformational changes occur in sodium channels before toxin binding (e.g., removal of inactivation: Chandler and Meves, 1970a–c; see below), they will also occur after toxin binding, although they may be modified by the toxins.

Under our experimental conditions, the largest observed difference between the GTX and VTD removal of inactivation behavior was in the time needed for this activation to reach a steady state. While VTD was essentially at equilibrium by 4 s, GTX-modified channels did not reach equilibrium for at least 30 s. The estimated $K_{1/2}$'s of toxin binding are not consistent with the assignation of these time-dependent differences to the experimental toxin concentrations alone. Instead, it appears that GTX binding equilibrates more slowly (tens of seconds) than VTD (seconds) due to slower association and dissociation rates, as reflected in the longer duration channel openings and closings observed with GTX. If so, then the shorter duration closings observed with GTX may be similar to the short closings of BTX-modified channels (Recio-Pinto et al., 1987) and reflect primarily transitions between modified open and inactive states.

In contrast to GTX and VTD, the most potent toxin of this group, BTX ($K_{1/2} \sim 0.7$ μM; Catterall, 1977), modifies eel electroplax channels with an apparent voltage- and concentration-independent fractional open time of 0.9–0.95 at all potentials more

depolarized than the activation gating region (Levinson et al., 1986; Recio-Pinto et al., 1987). Either BTX binding is not voltage dependent, or it dissociates too slowly or associates too rapidly for its observation in our experiments.

Evidence for a slow dissociation of BTX (much greater than VTD dissociation, and lasting >1 h at room temperature) has been reported from other laboratories (Catterall, 1975; Khodorov and Revenko, 1979). In planar bilayer studies, Green, Weiss, and Anderson (1987a) estimated the average BTX residence time to be ~250 min at room temperature. If the dissociation rate of BTX is this slow, then the lack of measurable voltage-dependent behavior in our experiments could be due to the short potential durations (seconds to minutes) relative to the BTX off rates (hours).

From these experimental considerations then, the three toxins can be ranked in order of residence times as: BTX > GTX > VTD. An examination of the toxin modifications of single channel conductance and activation gating with regard to this scheme is presented next.

Modified Sodium Channel Conductances and Activation

A summary of the conductance and activation properties of eel sodium channels modified with BTX, GTX, or VTD is given in Table II. In all cases, the I-V

TABLE II

Toxin	G	G^+	$G_{1/2}$	$V_{1/2}$
	pS	pS	pS	mV
BTX*	25	NF	12	−70
GTX	15	40–55	7	−90
VTD‡	12	NF	5	NF
Unmodified§	40	—	—	+4.4

*Recio-Pinto et al. (1987).
‡Duch et al. (1989).
§Shenkel and Sigworth (1991).
G is the predominant conductance measured; G^+ is the higher conductance state; $G_{1/2}$ is the smaller conductance; $v_{1/2}$ is the midpoint of activation gating; NF, not found.

relationships of the conductances are approximately linear and symmetrical between −100 and +100 mV.

The larger, 40–55-pS conductance found with GTX was not found with VTD- or BTX-modified channels. The relevance of this larger conductance state to toxin–channel interactions is discussed below.

GTX- and BTX-modified channels exhibited measurable activation gating behaviors, with GTX activation shifted ~20 mV in the hyperpolarized direction relative to BTX-modified channels. This shift may have been an artifact of the method used to examine the gating, selecting primarily for channels that gate at more negative (hyperpolarized) potentials, while channels that gate at less negative potentials were closed by channel inactivation before they could be observed. If so, this would suggest a much wider range of GTX-modified midpoints than observed with BTX. However, BTX-modified channels having such negative gating midpoints were rarely observed (Recio-Pinto et al., 1987). In addition, the frequency of the GTX-modified closed—

open transitions in this potential range was notably slower than in the presence of BTX, again indicating a difference in gating behavior.
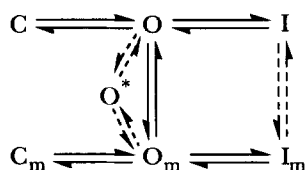
Activation gating of VTD-modified channels was not observed in any of our experiments, including the hyperpolarization of membranes to −160 mV. VTD-modified gating may be cut off too quickly by channel inactivation (and/or toxin unbinding) for recording in planar bilayers. Less likely is the possibility that VTD-modified activation gating is missing, as its presence has been described in other systems (Khodorov, 1985; Strichartz et al., 1987) and occurs at much more negative potentials than BTX-modified activation.

Thus, comparing toxin-modified conductances (picosiemens) and activation (more depolarized $V_{1/2}$) properties with those of unmodified eel channels, the ranking obtained is: unmodified > BTX > GTX > VTD, although VTD activation gating of electroplax channels has not yet been measured in bilayers (see, however, Castillo, Villegas, and Recio-Pinto, 1992). This order is the same found when the toxins were ranked according to slower dissociation rates.

Catterall (1977), using radiolabeled tracer uptake studies in neuroblastoma cells to compare the toxins according to the fraction of channels activated (i.e., ability to overcome inactivation) at saturating toxin concentrations, also ranked the toxins in this same order: BTX (0.95) > GTX (0.51) > VTD (0.08). Unmodified channels (which are almost completely inactivated during steady-state depolarization) would rank lower than VTD. In general, then, it appears that the stronger activators cause both less perturbation of the open and resting unmodified sodium channel states, and greater dissociation of inactivation from these states. The less perturbed the open and resting unmodified channel conformations are by the toxin interactions, then, the more stable the toxin-bound open state of the channel becomes. This is reflected in the longer residence times (BTX > GTX > VTD) of toxin binding.

Mechanism of Toxin Binding to the Sodium Channel

A model of toxin binding to the channel which fits both the equilibrium activation behavior of the toxins (Catterall, 1977) and the measured kinetics of toxin (VTD) interaction with the channel in voltage (Sutro, 1986; Rando, 1989) and patch (Sigel, 1987; Barnes and Hille, 1988) clamp studies was described by Barnes and Hille (1988; solid equilibria lines):

$$
\begin{array}{ccccc}
C & \rightleftharpoons & O & \rightleftharpoons & I \\
 & & \Updownarrow & & \Updownarrow \\
 & & O^* & & \\
 & & \Downarrow & & \\
C_m & \rightleftharpoons & O_m & \rightleftharpoons & I_m
\end{array}
$$

From this model, it can be seen that the modified open state of the channel (O_m) can be reached from three separate conformations: (a) the closed, modified conformation of the channel (C_m); (b) the open, unmodified channel (O); and (c) the inactivated, modified state of the channel (I_m). Our results are consistent with this description of

three separate pathways leading to the modified open state of the channel, but may not fit well with all of its details.

In accord with this model, our channel records indicate that the GTX-modified open state (16 pS) can apparently be reached from at least three separate conformations. Transitions from the closed (resting) state are indicated in the activation gating of the channel. In addition, the GTX-modified open state could apparently be reached from an inactive state of the channel, as well as from the large conducting (40–55 pS) state (Figs. 4–6).

Which state of the channel corresponds to this large conductance state? Its single channel conductance is similar to that found with patch recordings of unmodified eel electroplax sodium channels (Shenkel and Sigworth, 1991). It may therefore represent sodium channels that spontaneously open through the transient removal of inactivation (O). However, these large conductances were not observed in the absence of GTX, or in the presence of VTD, where channels are known to be in the membrane while the toxin is not always bound to them. This transiently open conformation of the channel thus appears to be a toxin-modified state of the channel, and may represent the brief stabilization of this open state by GTX before the more stable 15-pS conductance state is reached. These openings would thus occur between the channel's unmodified open state (O) and its modified open conformation (O_m). This pathway is represented as O* (dashed equilibrium lines) in the scheme above.

In support of such a mechanism, Chandler and Meves (1970a–c) have described an incompleteness of inactivation of squid axon sodium channels which increased with membrane depolarization (see Fig. 11 in Chandler and Meves, 1970c), similar to the observed voltage dependence of the large conductance transitions found in this study. In addition, we previously reported (Duch and Levinson, 1987b) that reconstituted eel channels spontaneously open from the inactive state in the absence of activating toxins. Subsequently, Cooper and Agnew (1989) reported that this spontaneous behavior occurred primarily at depolarized membrane potentials, in agreement with the voltage dependence of the large conductance bursts recorded here.

Alternatively, these openings might occur between the modified, inactivated state of the channel and its modified open state. In this case, every modified channel opening and closing would be preceded by a transient visit to a larger conducting state. Although our experiments do not have the frequency resolution to settle this question, bilayer recordings of BTX-modified channels at higher frequencies (Hartshorne, Keller, Talvenheimo, Catterall, and Montal, 1985) did not show evidence of large conductance either before or after the brief channel closings (presumably to a modified, inactive state). In addition, patch clamped, VTD-modified sodium channels (Sigel, 1987; Barnes and Hille, 1988) recorded at much higher frequencies did not give rise to similar conductances before all inactivation events.

The most important modification to the scheme of Barnes and Hille (1988), and also suggested by them, stems from the finding that the large conductance open state occurred asymmetrically before the 16-pS conductance state was reached and before it closed. In other words, if there were only one path for toxin binding and unbinding, the fraction of channel openings and closings preceded or followed by the large open state should be the same regardless of where in the above scheme these openings occurred. Instead, the large open state occurred twice as frequently before the 16-pS

openings as before the closings. Although several kinetic schemes could account for this behavior, the simplest is represented by inclusion of the dashed molecular transitions in the above binding scheme. In this case, the toxin could also unbind from the modified, inactive state (I_m), and under certain circumstances, also bind to the unmodified inactive state of the channel (I).

From such a model, it is easy to picture where voltage-dependent channel conformational changes could occur to affect toxin binding. As described by Chandler and Meves, (1970*a–c*), the h_2 kinetics of inactivation removal (the transition from I to O) are voltage dependent. Since GTX and VTD bind most readily to the open conformation of the channel, their binding site would be increasingly available at depolarized potentials. In a parallel manner, the equilibrium between the I_m and O_m states of the channel–toxin complex might also be voltage dependent.

In summary, we have compared the modification of sodium channel conductance, activation gating, and removal of inactivation by the lipid-soluble neurotoxins BTX, GTX, and VTD. The removal of inactivation appears to be the most relevant modification with regard to toxin potency. The observed voltage dependence of the removal of inactivation of GTX- and VTD-modified channels appears to result from the voltage-dependent binding of these toxins to the sodium channel, with the apparent affinity of toxin activation increasing with membrane depolarization. This voltage-dependent binding may result from the voltage-dependent availability of the receptor binding site, as proposed by Sutro (1986). These results, and those in our previous two papers, thus provide a picture of toxin modification in which the toxins dissociate channel inactivation from other channel properties and act to stabilize both the open and resting conformations of the channel. If this toxin interaction scheme is correct, it may become possible to design a compound that stabilizes the open state of the channel even more than BTX, and thereby gain structural information about the open, unmodified conformation of the sodium channel structure.

APPENDIX

Assuming that there is only one toxin bound per channel (Catterall, 1977), it is possible to determine the $K_{1/2}$ of toxin interaction with the channel from the binding equilibrium equation when two toxin concentrations are used for the determinations. The binding equilibrium equation states:

$$a = [T][NaCh]/(K_{1/2} + [T])$$ (A1)

where [T] is the concentration of alkaloid toxin, a is the concentration of toxin-bound channel receptors, [NaCh] is the total concentration of sodium channel present (bound and free), and $K_{1/2}$ is the concentration of toxin where half of the channels are activated. The concentration of toxin-bound channels includes both channels that are open (o) and channels that are closed (c; either resting or inactivated). At any potential, therefore:

$$a = o + c$$ (A2)

and, at each potential (at equilibrium):

$$o/c = x$$ (A3)

where x depends on potential but not on toxin concentration. Substituting and rearranging then gives:

$$a = o(1 + 1/x) = [T][NaCh]/(K_{1/2} + [T])\qquad(A4)$$

Comparing channel activation between two toxin concentrations at any given potential, then, the equation becomes:

$$a_1/a_2 = o_1/o_2 = \{[T_1][NaCh_1]/(K_{1/2} + [T_1])\}/\{[T_2][NaCh_2]/(K_{1/2} + [T_2])\}$$

where a_1 and a_2 represent the toxin-bound channel concentrations, and o_1/o_2 the concentration of toxin-bound open channels at $[T_1]$ and $[T_2]$, respectively. Both $[T_1]$ and $[T_2]$ are known, and (o_1/o_2) can be calculated from the ratio of the time-averaged conductances measured at each toxin concentration. Although the absolute concentration of channel present is not known, if the measurements are made on the same membrane, $[NaCh_1]$ and $[NaCh_2]$ will be equal and cancel in division.

REFERENCES

Barnes, S., and B. Hille. 1988. Veratridine modifies open sodium channels. *Journal of General Physiology.* 91:421–433.

Brown, G. B. 1988. Batrachotoxin: a window on the allosteric nature of the voltage-sensitive sodium channel. *International Review of Neurobiology.* 29:77–116.

Castillo, C., R. Villegas, and E. Recio-Pinto. 1992. Alkaloid-modified sodium channels from lobster walking leg nerves in planar lipid bilayers. *Journal of General Physiology.* 99:897–930.

Catterall, W. A. 1975. Activation of the action potential Na$^+$ ionophore of cultured neuroblastoma cells by veratridine and batrachotoxin. *Journal of Biological Chemistry.* 250:4053–4059.

Catterall, W. A. 1977. Activation of the action potential Na$^+$ ionophore by neurotoxins: an allosteric model. *Journal of Biological Chemistry.* 252:8669–8676.

Catterall, W. A. 1980. Neurotoxins that act on voltage-sensitive sodium channels in excitable membranes. *Annual Review of Pharmacology and Toxicology.* 20:15–43.

Chandler, W. K., and H. Meves. 1970a. Sodium and potassium currents in squid axons perfused with fluoride solution. *Journal of Physiology.* 211:623–652.

Chandler, W. K., and H. Meves. 1970b. Evidence for two types of sodium conductance in axons perfused with sodium fluoride solution. *Journal of Physiology.* 211:653–678.

Chandler, W. K., and H. Meves. 1970c. Rate constants associated with changes in sodium conductance in axons perfused with fluoride solutions. *Journal of Physiology.* 211:679–705.

Cooper, E. C., and W. S. Agnew. 1989. Reconstituted voltage-sensitive sodium channels from eel electroplax: activation of permeability by quaternary lidocaine, n-bromoacetamide, and n-bromosuccinimide. *Journal of Membrane Biology.* 111:253–264.

Duch, D. S., and S. R. Levinson. 1987a. Neurotoxin-modulated uptake of sodium by highly purified preparations of the electroplax tetrodotoxin-binding glycopeptide reconstituted into lipid vesicles. *Journal of Membrane Biology.* 98:43–55.

Duch, D. S., and S. R. Levinson. 1987b. Spontaneous opening at zero membrane potential of sodium channels from eel electroplax reconstituted into lipid vesicles. *Journal of Membrane Biology.* 98:57–68.

Duch, D. S., S. R. Levinson, and B. W. Urban. 1991. Grayanotoxin modification of purified eel electroplax sodium channels in planar bilayers. *Biophysical Journal.* 59:259a. (Abstr.)

Duch, D. S., E. Recio-Pinto, C. Frenkel, S. R. Levinson, and B. W. Urban. 1989. Veratridine modification of the purified sodium channel α-polypeptide from eel electroplax. *Journal of General Physiology.* 94:813–831.

Duch, D. S., E. Recio-Pinto, C. Frenkel, and B. W. Urban. 1988. Human brain sodium channels in bilayers. *Molecular Brain Research.* 4:171–177.

Green, W. N., L. B. Weiss, and O. S. Andersen. 1987a. Batrachotoxin-modified sodium channels in planar bilayers. Ion permeation and block. *Journal of General Physiology.* 89:841–872.

Green, W. N., L. B. Weiss, and O. S. Andersen. 1987b. Batrachotoxin-modified sodium channels in planar bilayers. Characterization of saxitoxin- and tetrodotoxin-induced channel closures. *Journal of General Physiology.* 89:873–903.

Hartshorne, R. P., B. U. Keller, J. A. Talvenheimo, W. A. Catterall, and M. Montal. 1985. Functional reconstitution of the purified brain sodium channel in planar lipid bilayers. *Proceedings of the National Academy of Sciences, USA.* 82:240–244.

Khodorov, B. I. 1985. Batrachotoxin as a tool to study voltage-sensitive sodium channels of excitable membranes. *Progress in Biophysics and Molecular Biology.* 45:57–148.

Khodorov, B. I., and S. V. Revenko. 1979. Further analysis of the mechanisms of action of batrachotoxin on the membrane of myelinated nerve. *Neuroscience.* 4:1315–1330.

Levinson, S. R., D. S. Duch, B. W. Urban, and E. Recio-Pinto. 1986. The sodium channel from Electrophorus electricus. *Annals of the New York Academy of Sciences.* 479:162–178.

Moczydlowski, E., S. Hall, S. S. Garber, G. S. Strichartz, and C. Miller. 1984. Voltage-dependent blockade of muscle Na^+ channels by guanidinium toxins. Effect of toxin charge. *Journal of General Physiology.* 84:687–704.

Narahashi, T., and I. Seyama. 1974. Mechanism of nerve membrane depolarization caused by grayanotoxin I. *Journal of Physiology.* 242:471–487.

Rando, T. A. 1989. Rapid and slow gating of veratridine-modified sodium channels in frog myelinated nerve. *Journal of General Physiology.* 93:43–65.

Recio-Pinto, E., D. S. Duch, S. R. Levinson, and B. W. Urban. 1987. Purified and unpurified sodium channels from Eel electroplax in planar bilayers. *Journal of General Physiology.* 90:375–395.

Shenkel, S., and F. J. Sigworth. 1991. Patch recordings from the electrocytes of *Electrophorus electricus. Journal of General Physiology.* 97:1013–1041.

Sigel, E. 1987. Effects of veratridine on single neuronal sodium channels expressed in *Xenopus* oocytes. *Pflügers Archiv.* 410:112–120.

Strichartz, G., T. Rando, and G. K. Wang. 1987. An integrated view of the molecular toxinology of sodium channel gating in excitable cells. *Annual Review of Neuroscience.* 10:237–267.

Sutro, J. B. 1986. Kinetics of veratridine action on Na channels of skeletal muscle. *Journal of General Physiology.* 87:1–24.

Ulbricht, W. 1969. The effect of veratridine on excitable membranes of nerve and muscle. *Ergebnisse der Physiologie.* 61:18–71.